

DFTT 15/03

SHEP-03-11

July 2003

## One-loop weak corrections to the $b\bar{b}$ cross section at TeV energy hadron colliders

E. Maina<sup>a,1</sup>, S. Moretti<sup>b,2</sup>, M.R. Nolten<sup>b,3</sup> and D.A. Ross<sup>b,4</sup>

*a) Dipartimento di Fisica Teorica and Sezione INFN, Università di Torino,  
Via Pietro Giuria 1, 10125 Torino, Italy*

*2) School of Physics & Astronomy, University of Southampton,  
Highfield, Southampton SO17 1BJ, UK*

### Abstract

We investigate one-loop weak corrections to the production cross section of two  $b$ -jets at Tevatron and Large Hadron Collider (LHC). We establish that they are small at inclusive level but dominant in exclusive observables that have a non-trivial dependence on the helicity structure of the hard subprocesses. Such effects can serve as a test of the Standard Model (SM) and, conversely, they should be taken into account in future experimental analyses aiming at extracting possible signals of new physics.

Keywords: Electro-Weak Effects, Loop Calculations, Bottom Quarks, Hadron Colliders

---

<sup>1</sup>maina@to.infn.it

<sup>2</sup>stefano@hep.phys.soton.ac.uk

<sup>3</sup>mrn@hep.phys.soton.ac.uk

<sup>4</sup>dar@hep.phys.soton.ac.uk

## Introduction

It has already been clearly established [1]–[28] that large Sudakov logarithms arising at TeV energy scales as a consequence of a non-cancellation between real and virtual contributions can enhance the effects of Electro-Weak (EW) corrections in electron-positron scattering, so that the latter grow as  $\alpha_{\text{EW}}^n \log^{2n}(s/M_W^2)$  at the  $n$ -th perturbative order even in fully inclusive observables, where  $s_{e^+e^-}$  is the collider centre-of-mass (CM) energy squared and  $M_W$  the  $W$  boson mass. Eventually, they can even surpass the corrections generated in QCD: e.g., in the total hadronic cross section at  $\sqrt{s_{e^+e^-}} \approx 800$  GeV and above.

The reason for this is intimately related to the violation of the Bloch-Nordsieck theorem occurring in non-Abelian theories whenever the initial state has a finite (weak) isospin charge<sup>5</sup>, as dictated by the given beam configuration. This is immediately evident for leptonic colliders, as the Sudakov logarithms present in  $e^+e^-$  scattering would cancel against those originating in  $e^+\nu_e$  and  $\bar{\nu}_e e^-$  collisions (the (anti)neutrinos are the isospin partners of the electron/positrons), a condition which is clearly impossible to satisfy experimentally. One can view the mechanism rather intuitively from a diagrammatic perspective. In short, virtual  $W$  corrections simply multiply the leading-order (LO) scattering matrix elements, thus being proportional to  $\sigma_{e^+e^-}$ , while the real emission of a  $W$  boson does change the isospin of the incoming electron/positron and turns it into a(n) (anti)neutrino, so that the corrections here are proportional to  $\sigma_{e^+\nu_e}$  and  $\sigma_{\bar{\nu}_e e^-}$ .

Evidently, this does not occur for the case of real and virtual  $Z$  boson corrections (or photons, for that matters). The source of the large logarithms is then in principle manifest only in the case of  $W$  boson corrections. In practice, though, one should recall that both  $W$  and  $Z$  real bosons are unstable and decay into high transverse momentum leptons and/or jets, which are normally captured by the detectors. In the definition of an exclusive cross section, one may then remove events with such additional particles. Ultimately, other than being a second source of Bloch-Nordsieck violation for the case of  $W$  corrections, this merely experimental procedure will also spoil the cancellations between real and virtual contributions in the case of  $Z$  bosons, simply because the former are not included in the definition of the measured quantity.

The leading, double-logarithmic, angular-independent weak logarithmic corrections are universal, i.e. they depend only on the identities of the external particles. Both leading and subleading corrections are finite (unlike in QED and QCD), as the masses of the  $W$  and  $Z$  gauge bosons provide a physical cut-off for the otherwise divergent infrared behaviour. In some instances large cancellation between angular-independent and angular-dependent corrections [14] and between leading and subleading corrections [23] have been found at TeV energies. It is therefore of paramount

---

<sup>5</sup>The problem is in principle present also in QCD, with respect to the colour charge; in practice, however, it has no observable consequences, because of the final averaging of the colour degrees of freedom of the incoming partons, forced by their confinement into colourless hadrons.

importance to study the full set of fixed order weak corrections in order to establish the relative size of the different contributions at the energy scales which will be probed at TeV scale machines.

Furthermore, weak contributions can be isolated in a gauge-invariant manner from purely Electro-Magnetic (EM) (or QED) effects [3], [7]–[9], which may or may not be included in the calculation, depending on the observable being studied and the aimed at accuracy. In view of all such arguments, it is then legitimate and topical to investigate the importance of higher-order weak effects at TeV scale hadronic colliders [14], such as Tevatron ( $\sqrt{s_{p\bar{p}}} = 2$  TeV) and LHC ( $\sqrt{s_{pp}} = 14$  TeV).

Some further considerations are however in order in the hadronic context. First, one should recall that hadron-hadron scatterings ( $pp, p\bar{p}$ ) involve valence (or sea) partons of opposite isospin in the same process. Thus the above-mentioned cancellations may potentially be restored. For example, in  $p\bar{p}(pp)$  scatterings one finds both  $u\bar{u}(uu)$  and  $u\bar{d}(ud)$  subprocess contributions to the total hadronic cross section, which tend to balance each other, this effect being actually modulated by the Parton Distribution Functions (PDFs). Secondly, several crossing symmetries among the involved partonic subprocesses can also easily lead to more cancellations. Thirdly, whether or not these two mechanisms take place, spin asymmetries due to weak effects would always be manifest in some observables, since QCD has a trivial helicity structure (just like QED).

The purpose of this paper is that of establishing the importance of one-loop weak effects in  $b$ -jet production at Tevatron and LHC. This is a pressing problem, as the  $p_T$  distribution of Tevatron data for  $b$ -quark production shows a clear disagreement with the theory [29], now known to next-to-leading order (NLO) accuracy in QCD [30]<sup>6</sup>, even after all uncertainties related to the definition of the cross section [31] and the extraction of the  $b$ -quark fragmentation function are properly taken into account [32]. In order to avoid such uncertainties, we consider in this paper the cross section for di-jet production for which each jet contains a  $b(\bar{b})$ -quark. Data from Run 2 is also expected to be presented in this format [29]. Comparisons of such  $b$ -jet cross sections from Run 1 with NLO QCD [33] show a less severe discrepancy than in the case of  $b$ -quark distributions. The comparison between theory and  $b$ -quark/jet data is eventually expected to continue at LHC with much higher precision [34].

## Production of $b$ -jets at Tevatron and LHC

Even if the discrepancy referred to at the end of the previous section may not appear alarming at this stage, it is conceivable that the higher statistics available after Run 2 will afford the possibility of looking at more exclusive observables, in order to understand whether the difference may be due to some possible new physics effects, such as, e.g.,  $W'$  and  $Z'$  gauge bosons [35]. In this respect, it is natural to turn to quantities which are insensitive to QCD effects, such as the aforementioned

---

<sup>6</sup>Also the subleading LO tree-level contributions from EW interactions have been calculated.

spin induced asymmetries in the cross section. From this point of view, the knowledge of the weak effects described above would be of paramount importance, even if their overall contribution to the inclusive cross section should turn out to be negligible.

After Run 2 at Tevatron, the accumulated statistics will be sufficient to select hadronic samples with two  $b$ -jets and to establish their charge as well: e.g., by extracting two displaced vertices and measuring the charge of one of the (at least two) associated jets, via a high  $p_T$  lepton selection or jet charge reconstruction. This will enable one to define the usual ‘forward-backward asymmetry’ for  $b$ -jets also at hadronic colliders, hereafter denoted by  $A_{\text{FB}}^7$ . Unfortunately, because of the symmetric beam configuration at LHC, one cannot define the forward-backward asymmetry in this case. Pure QCD contributions through orders  $\alpha_S^2$  and  $\alpha_S^3$  to such a quantity are negligible at Tevatron compared to the tree-level EW ones, which are of order  $\alpha_{\text{EW}}^2$ . We set out here to compute one-loop virtual effects to  $b\bar{b}$  production through order  $\alpha_S^2\alpha_{\text{EW}}$ , which have then formally a similar strength to the purely EW ones, given that  $\alpha_S^2 \sim \alpha_{\text{EW}}$  at TeV energies.

Before proceeding, we should like to clarify here that we will only include (in the language of Ref. [31]) ‘flavour creation’ contributions and neglect both the ‘flavour excitation’ and ‘shower/fragmentation’ ones. While this is certainly not justified in the total inclusive  $b$ -cross section [31], it is entirely appropriate for the  $b\bar{b}$  one that we will be using in the definition of  $A_{\text{FB}}$ , for which we will require ‘two’ high  $p_T$   $b$ -jets (thus depleting the ‘flavour excitation’ terms) tagged in opposite hemispheres (thus suppressing the ‘shower/fragmentation’ contributions). Finally, as anticipated in the previous discussion, we will neglect including QED corrections at this stage of our computation (this is indeed a gauge-invariant procedure, as we have explicitly verified), since we will ultimately be most interested in the forward-backward asymmetry, to which pure EM terms contribute negligibly.

## Partonic contributions to the $pp/p\bar{p} \rightarrow b\bar{b}$ cross section

The inclusive  $b$ -jet cross section at both Tevatron and LHC is dominated by the pure QCD contributions  $gg \rightarrow b\bar{b}$  and  $q\bar{q} \rightarrow b\bar{b}$ , known through order  $\alpha_S^n$  for  $n = 2, 3$ . Of particular relevance in this context is the fact that for the flavour creation mechanisms no  $\alpha_S\alpha_W$  tree-level contributions are allowed, because of colour conservation: i.e.,

$$\begin{array}{c} q \\ \swarrow \\ \text{---} \\ \searrow \\ \bar{q} \end{array} \begin{array}{c} b \\ \swarrow \\ \text{---} \\ \searrow \\ \bar{b} \end{array} \quad * \quad \left[ \begin{array}{c} q \\ \swarrow \\ \text{---} \\ \searrow \\ \bar{q} \end{array} \begin{array}{c} b \\ \swarrow \\ \text{---} \\ \searrow \\ \bar{b} \end{array} \right]^\dagger = 0, \quad (1)$$

where the wavy line represents a  $Z$  boson (or a photon) and the helical one a gluon. Tree-level asymmetric terms through the order  $\alpha_{\text{EW}}^2$  are however finite, as they are given by non-zero quark-

<sup>7</sup>In this respect, it is intriguing to recall the long-standing disagreement between data and SM for such a quantity, as seen at LEP and SLD [36], as well as several other observables involving  $b$ -quarks/jets, both at collider and fixed target experiments [37].

antiquark initiated diagrams such as the one above wherein the gluon is replaced by a  $Z$  boson (or a photon). The latter are the leading contribution to the forward-backward asymmetry (more precisely, those graphs containing one or two  $Z$  bosons are, as those involving two photons are subleading in this case, even with respect to the pure QCD contributions).

Here, we will compute one-loop and (gluon) radiative contributions through the order  $\alpha_S^2\alpha_W$ , which – in the case of quark-antiquark induced subprocesses – are represented schematically by the following diagrams:

$$\begin{aligned}
& \begin{array}{c} q \quad b \\ \diagdown \quad / \\ \text{---} \text{---} \text{---} \\ / \quad \diagdown \\ \bar{q} \quad \bar{b} \end{array} * \left[ \begin{array}{c} q \quad b \\ \diagdown \quad / \\ \text{---} \text{---} \text{---} \\ / \quad \diagdown \\ \bar{q} \quad \bar{b} \end{array} \right]^\dagger + \text{crossed box} + \\
& \begin{array}{c} q \quad b \\ \diagdown \quad / \\ \text{---} \text{---} \text{---} \\ / \quad \diagdown \\ \bar{q} \quad \bar{b} \end{array} * \left[ \begin{array}{c} q \quad b \\ \diagdown \quad / \\ \text{---} \text{---} \text{---} \\ / \quad \diagdown \\ \bar{q} \quad \bar{b} \end{array} \right]^\dagger + \text{crossed box} + \\
& \begin{array}{c} q \quad b \\ \diagdown \quad / \\ \text{---} \text{---} \text{---} \\ / \quad \diagdown \\ \bar{q} \quad \bar{b} \end{array} * \left[ \begin{array}{c} q \quad b \\ \diagdown \quad / \\ \text{---} \text{---} \text{---} \\ / \quad \diagdown \\ \bar{q} \quad \bar{b} \end{array} \right]^\dagger + \text{other three vertices} + \\
& + \text{all self-energies} + \\
& \begin{array}{c} q \quad b \\ \diagdown \quad / \\ \text{---} \text{---} \text{---} \\ / \quad \diagdown \\ \bar{q} \quad \bar{b} \end{array} * \left[ \begin{array}{c} q \quad b \\ \diagdown \quad / \\ \text{---} \text{---} \text{---} \\ / \quad \diagdown \\ \bar{q} \quad \bar{b} \end{array} \right]^\dagger + \text{gluon permutations.} \tag{2}
\end{aligned}$$

The gluon bremsstrahlung graphs are needed in order to cancel the infinities arising in the virtual contributions when the intermediate gluon becomes infrared. Furthermore, one also has to include  $\alpha_S^2\alpha_W$  terms induced by gluon-gluon scattering, that is, interferences between the graphs displayed in Fig. 1 of Ref. [38] and the tree-level ones for  $gg \rightarrow b\bar{b}$ . In the remainder of this paper, we will assume  $m_b = 0$  and  $m_t = 175$  GeV (with  $\Gamma_t = 1.55$  GeV): the top-quark enters the vertices and self-energies of the diagrams in (2) as well as the boxes (in additions to self-energies and vertices themselves) in Fig. 1 of Ref. [38], whenever a virtual  $W$  exchange occurs. The  $Z$  mass used was  $M_Z = 91.19$  GeV and was related to the  $W$  mass,  $M_W$ , via the SM formula  $M_W = M_Z \cos \theta_W$ , where  $\sin^2 \theta_W = 0.232$ . (Corresponding widths were  $\Gamma_Z = 2.5$  GeV and  $\Gamma_W = 2.08$  GeV.) For  $\alpha_S$  we have used the one- or two-loop expressions as specified below, with  $\Lambda_{\overline{\text{MS}}}^{(n_f=4)}$  set according to the PDFs used.

Some of the diagrams contain ultraviolet divergences. These have been subtracted using the ‘modified’ Minimal Subtraction ( $\overline{\text{MS}}$ ) scheme at the scale  $\mu = M_Z$ . Thus the couplings are taken to be those relevant for such a subtraction: e.g., the EM coupling,  $\alpha_{\text{EM}} \equiv \alpha_{\text{EW}} \sin^2 \theta_W$ , has been taken to be  $1/128$  at the above subtraction point. The one exception to this renormalisation scheme has been the case of the self-energy insertions on external fermion lines, which have been subtracted on mass-shell, so that the external fermion fields create or destroy particle states with the correct normalisation.

Infrared divergences occur when the virtual or real (bremsstrahlung) gluon is either soft or collinear with the emitting parton. It is because we are considering  $b$ -jets which include a possible gluon parallel to the  $b$ -quark rather than open  $b$ -quark production that the collinear divergences cancel, this way removing the logarithmic dependence on the  $b$ -quark mass which was investigated and resummed in the analysis of Ref. [39]. Moreover, in our case the collinear divergences cancel amongst themselves. This can be seen since by colour conservation only interferences between gluon emission from the initial and final state quarks are permitted. If the gluon is parallel to an initial (final) quark then from the collinear vertex it is contracted into its own momentum and the sum of amplitudes for a longitudinal gluon emitted from both final (initial) states cancels by virtue of a Ward identity. For virtual corrections, the infrared divergences arise from the box graphs and there is an equivalent cancellation of collinear divergences between the crossed and uncrossed boxes. This leaves the soft divergences which can be readily extracted and as expected cancel between the virtual corrections and bremsstrahlung emissions. Nevertheless, for the sake of numerical stability when carrying out the necessary numerical integration over phase space and convolution with the PDFs, it is preferable to use the formalism of Catani and Seymour [40], whereby corresponding dipole terms are subtracted from the bremsstrahlung contributions in order to render the phase space integral free of infrared divergences. The integration over the gluon phase-space of these dipole terms are performed analytically in  $d$ -dimensions, yielding pole terms which cancel explicitly against the pole terms of the box graphs.

Our expressions for each of the diagrams contain the complete helicity information from both the initial and final state. They have been calculated using FORM [41] and reproduced by an independent program based on FeynCalc [42]. The formulae have all been checked for gauge invariance. The full expressions for the contributions from all possible  $\alpha_S^2 \alpha_{\text{EW}}$  graphs are too lengthy to be reproduced here.

## Numerical results for Tevatron and LHC

We start our numerical investigation of the processes  $pp/p\bar{p} \rightarrow b\bar{b}$  by first computing the total cross section,  $\sigma(pp \rightarrow b\bar{b})$ , for Tevatron (Run 2). This can be found in Fig. 1 (top), as a function of the transverse momentum of the  $b$ -jet (or  $\bar{b}$ -jet) and decomposed in terms of the various subprocesses

discussed so far. (Hereafter, the pseudorapidity is limited between  $-2$  and  $2$  in the partonic CM frame.) The dominance at inclusive level of the pure QCD contributions is manifest, over the entire  $p_T$  spectrum. At low transverse momentum it is the gluon-gluon induced subprocess that dominates, with the quark-antiquark one becoming the strongest one at large  $p_T$ . The QCD  $K$ -factors, defined as the ratio of the  $\alpha_S^3$  rates to the  $\alpha_S^2$  ones are rather large, of order 2 and positive for the  $gg \rightarrow b\bar{b}$  subprocess and somewhat smaller for the  $q\bar{q} \rightarrow b\bar{b}$  case, which has a  $p_T$ -dependent sign<sup>8</sup>. The tree-level  $\alpha_{EW}^2$  terms are much smaller than the QCD rates, typically by three orders of magnitude, with the exception of the  $p_T \approx M_Z/2$  region, where one can appreciate the onset of the  $Z$  resonance in  $s$ -channel. All above terms are positive. The  $\alpha_S^2\alpha_{EW}$  subprocesses display a more complicated structure, as their sign can change over the transverse momentum spectrum considered, and the behaviour is different in  $q\bar{q} \rightarrow b\bar{b}(g)$  from  $gg \rightarrow b\bar{b}$ . Overall, the rates for the  $\alpha_S^2\alpha_{EW}$  channels are smaller by a factor of four or so, compared to the tree-level  $\alpha_{EW}^2$  cross sections. Fig. 1 (bottom) shows the percentage contributions of the  $\alpha_S^3$ ,  $\alpha_{EW}^2$  and  $\alpha_S^2\alpha_{EW}$  subprocesses, with respect to the leading  $\alpha_S^2$  ones, defined as the ratio of each of the former to the latter<sup>9</sup>. The  $\alpha_S^2\alpha_{EW}$  terms represent a correction of the order of the fraction of percent to the leading  $\alpha_S^2$  terms. Clearly, at inclusive level, the effects of the Sudakov logarithms are not large at Tevatron, this being mainly due to the fact that in the partonic scattering processes the hard scale involved is not much larger than the  $W$  and  $Z$  masses.

Next, we study the above mentioned forward-backward asymmetry, defined as follows:

$$A_{\text{FB}} = \frac{\sigma_+(p\bar{p} \rightarrow b\bar{b}) - \sigma_-(p\bar{p} \rightarrow b\bar{b})}{\sigma_+(p\bar{p} \rightarrow b\bar{b}) + \sigma_-(p\bar{p} \rightarrow b\bar{b})}, \quad (3)$$

where the subscript  $+$ ( $-$ ) identifies events in which the  $b$ -jet is produced with polar angle larger (smaller) than 90 degrees respect to one of the two beam directions (hereafter, we use the proton beam as positive  $z$ -axis). The polar angle is defined in the CM frame of the hard partonic scattering. Notice that we do not implement a jet algorithm, as we integrate over the entire phase space available to the gluon. In practice, this corresponds to summing over the two- and three-jet contributions that one would extract from the application of a jet definition. The solid curve in Fig. 2 (top) represents the sum of the tree-level contributions only, that is, those of order  $\alpha_S^2$  and  $\alpha_{EW}^2$ , whereas the dashed one also includes the higher-order ones  $\alpha_S^3$  and  $\alpha_S^2\alpha_{EW}$ . (Recall that the contributions to the asymmetry due to the pure QED and QCD terms  $\alpha_{EM}^2$ ,  $\alpha_S^2$  and  $\alpha_S^3$  are negligible<sup>10</sup>.)

The effects of the one-loop weak corrections on this observable are extremely large, as they are not only competitive with, if not larger than, the tree-level weak contributions, but also of opposite

---

<sup>8</sup>Further notice that in QCD at NLO one also has (anti)quark-gluon induced (tree-level) contributions, which are of similar strength to those via gluon-gluon and quark-antiquark scattering but which have not been shown here.

<sup>9</sup>In the case of the  $\alpha_S^3$  corrections, we have used the two-loop expression for  $\alpha_S$  and a NLO fit for the PDFs, as opposed to the one-loop formula and LO set for the other processes (we adopted the GRV94 [43] PDFs with  $\overline{\text{MS}}$  parameterisation).

<sup>10</sup>And so would also be the one-loop  $\alpha_S^2\alpha_{EM}$  terms not computed here.

sign over most of the considered  $p_T$  spectrum. In absolute terms, the asymmetry is of order  $-4\%$  at the  $W$ ,  $Z$  resonance and fractions of percent elsewhere, hence it should comfortably be measurable after the end of Run 2.

Fig. 3 shows the same quantities as in Fig. 1, now defined at LHC energy. By a comparative reading, one may appreciate the following aspects. Firstly, the effects at LHC of the  $\alpha_S^2\alpha_{EW}$  corrections are much larger than the  $\alpha_{EW}^2$  ones already at inclusive level (see top of Fig. 3), as their absolute magnitude becomes of order  $-2\%$  or so at large transverse momentum (see bottom of Fig. 3): clearly, logarithmic enhancements are at LHC much more effective than at Tevatron energy scales<sup>11</sup>. Secondly, the overall production rates at the CERN collider are in general much larger than those at FNAL, because of the much larger gluon component of the proton.

## Conclusions

In summary, we should like to remark upon the following aspects of our analysis.

- Inclusive corrections to the  $b\bar{b}$  cross section due to one-loop weak interaction contributions through order  $\alpha_S^2\alpha_{EW}$  are small and undetectable at Tevatron, while becoming visible at LHC, because of the much larger cross section and luminosity available. In practice, the weak Sudakov logarithms are threshold suppressed at the FNAL collider while at the CERN machine they become sizable. In the former case then, they cannot explain the current data vs. theory discrepancy seen in the  $b$ -quark/jet cross sections.
- One-loop weak effects onto  $b$ -quark asymmetries (e.g., we have studied the forward-backward one) are found to be large at Tevatron, where they can be defined experimentally. Here, the forward-backward asymmetry is subject to large corrections because the tree-level (quark-antiquark) subprocesses are formally of the same order as the one-loop contributions (initiated by both quark-antiquark and gluon-gluon collisions), eventually being measurable if collider luminosity plans will turn out to be on schedule.

In conclusion, at both current and planned TeV scale hadronic colliders, one-loop weak effects from SM physics may be important and need to be taken into account particularly in order to extract possible signals of new physics from data.

## Acknowledgments

MRN, SM and DAR thanks the Department of Theoretical Physics at Torino University for hospitality while part of this work was being carried out. SM and DAR are grateful to Stefano Catani

---

<sup>11</sup>Further notice at LHC the dominance of the  $gg$ -induced one-loop terms, as compared to the corresponding  $q\bar{q}$ -ones (top of Fig. 3), contrary to the case of Tevatron, where they were of similar strength (top of Fig. 1).



and Mike Seymour for advice. SM thanks Matteo Cacciari for helpful discussions. This project was in part financed by the U.K. Particle Physics and Astronomy Research Council (PPARC), by the Italian Ministero dell'Istruzione, dell'Università e della Ricerca (MIUR) under contract 2001023713\_006, by the European Union under contract HPRN-CT-2000-00149 and by The Royal Society (London, UK) under the European Science Exchange Programme (ESEP), Grant No. IES-14468.

## References

- [1] M. Kuroda, G. Moulataka and D. Schildknecht, Nucl. Phys. **B350**, 25 (1991); G. Degrassi and A. Sirlin, Phys. Rev. **D46**, 3104 (1992); A. Denner, S. Dittmaier and R. Schuster, Nucl. Phys. **B452**, 80 (1995); A. Denner, S. Dittmaier and T. Hahn, Phys. Rev. **D56**, 117 (1997); A. Denner and T. Hahn, Nucl. Phys. **B525**, 27 (1998).
- [2] W. Beenakker, A. Denner, S. Dittmaier, R. Mertig and T. Sack, Nucl. Phys. **B410**, 245 (1993); Phys. Lett. **B317**, 622 (1993).
- [3] P. Ciafaloni and D. Comelli, Phys. Lett. **B446**, 278 (1999).
- [4] M. Ciafaloni, P. Ciafaloni and D. Comelli, Phys. Rev. Lett. **84**, 4810 (2000) .
- [5] M. Ciafaloni, P. Ciafaloni and D. Comelli, Phys. Rev. Lett. **87**, 211802 (2001).
- [6] M. Ciafaloni, P. Ciafaloni and D. Comelli, Nucl. Phys. **B613**, 382 (2001).
- [7] M. Beccaria, P. Ciafaloni, D. Comelli, F.M. Renard and C. Verzegnassi, Phys. Rev. **D61**, 073005 (2000).
- [8] M. Beccaria, F.M. Renard and C. Verzegnassi, Phys. Rev. **D63**, 053013 (2001).
- [9] M. Beccaria, F.M. Renard and C. Verzegnassi, Phys. Rev. **D64**, 073008 (2001).
- [10] A. Denner, talk given at the ' International Europhysics Conference on High Energy Physics', Budapest, Hungary, July 12-18, 2001.
- [11] A. Denner and S. Pozzorini, Eur. Phys. J. **C18**, 461 (2001).
- [12] A. Denner and S. Pozzorini, Eur. Phys. J. **C21**, 63 (2001).
- [13] S. Pozzorini, Ph.D. Dissertation, Universität Zürich (2001).
- [14] E. Accomando, A. Denner and S. Pozzorini, Phys. Rev. **D65**, 073003 (2002).
- [15] M. Melles, Phys. Lett. **B495**, 81 (2000).
- [16] M. Hori, H. Kawamura and J. Kodaira, Phys. Lett. **B491**, 275 (2000).
- [17] W. Beenakker and A. Werthenbach, Nucl. Phys. Proc. Suppl. **89**, 88 (2000).
- [18] W. Beenakker and A. Werthenbach, Phys. Lett. **B489**, 148 (2000).
- [19] W. Beenakker and A. Werthenbach, Nucl. Phys. **B630**, 3 (2002).
- [20] V.S. Fadin, L.N. Lipatov, A.D. Martin and M. Melles, Phys. Rev. **D61**, 094002 (2000).

- [21] P. Ciafaloni and D. Comelli, Phys. Lett. **B476**, 49 (2000).
- [22] J.H. Kühn, A. A. Penin and V. A. Smirnov, Eur. Phys. J. **C17**, 97 (2000).
- [23] J.H. Kühn, S. Moch, A.A. Penin and V.A. Smirnov, Nucl. Phys. **B616**, 286 (2001).
- [24] M. Melles, Phys. Rev. **D63**, 034003 (2001).
- [25] M. Melles, Phys. Rev. **D64**, 014011 (2001).
- [26] M. Melles, Phys. Rev. **D64**, 054003 (2001).
- [27] M. Melles, Phys. Rept. **375**, 219 (2003).
- [28] M. Melles, Eur. Phys. J. **C24**, 193 (2002).
- [29] See, e.g., R.K. Ellis et al., in preprint FERMILAB-Pub-01/197 (Chapter 9 and references therein).
- [30] P. Nason, S. Dawson and R.K. Ellis, Nucl. Phys. **B303**, 607 (1988); *ibidem*, **B327**, 49 (1989); W. Beenakker, H. Kuijf, W.L. van Neerven and J. Smith, Phys. Rev. **D40**, 54 (1989); W. Beenakker, W.L. van Neerven, R. Meng, G.A. Schuler and J. Smith, Nucl. Phys. **B351**, 507 (1991); M.L. Mangano, P. Nason and G. Ridolfi, Nucl. Phys. **B373**, 295 (1992).
- [31] R.D. Field, Phys. Rev. **D65**, 094006 (2002).
- [32] M. Cacciari and P. Nason, Phys. Rev. Lett. **89**, 122003 (2002); M. Cacciari, talk given at the workshop ‘Physics at TeV Colliders’, Les Houches, France, 26 May-6 June 2003: see <http://www.nikhef.nl/pub/theory/leshouches03talks/cacciari-b-excess.pdf>.
- [33] S. Frixione and M.L. Mangano, Nucl. Phys. **B483**, 321 (1997).
- [34] P. Nason, G. Ridolfi, O. Schneider, G.F. Tartarelli and P. Vikas (conveners), in proceedings of the workshop on ‘Standard Model Physics (and more) at the LHC’, Geneva 1999 (Pages 231–304 and references therein).
- [35] A. Bodek and U. Baur, Eur. Phys. J. **C21**, 607 (2001).
- [36] See, e.g.: <http://lepewwg.web.cern.ch/LEPEWWG/heavy/>.
- [37] S. Frixione, plenary talk at the ‘XXXIth International Conference on High Energy Physics (ICHEP 2002)’, Amsterdam, The Netherlands, 24-31 July 2002, Nucl. Phys. Proc. Suppl. **117**, 222 (2003).
- [38] J.E. Ellis, S. Moretti and D.A. Ross, JHEP **06**, 043 (2001).
- [39] M. Cacciari, M. Greco and P. Nason, JHEP **05**, 007 (1998); M. Cacciari and M. Greco, Nucl. Phys. **B421**, 530 (1994).
- [40] S. Catani and M.H. Seymour, Nucl. Phys. **B485**, 291 (1997); Erratum, *ibidem* **B510**, 503 (1997).
- [41] J.A.M. Vermaseren, preprint NIKHEF-00-032 [math-ph/0010025].
- [42] J. Küblbeck, M. Böhm and A. Denner, Comput. Phys. Commun. **64**, 165 (1991).
- [43] M. Glück, E. Reya and A. Vogt, Z. Phys. **C67**, 433 (1995).

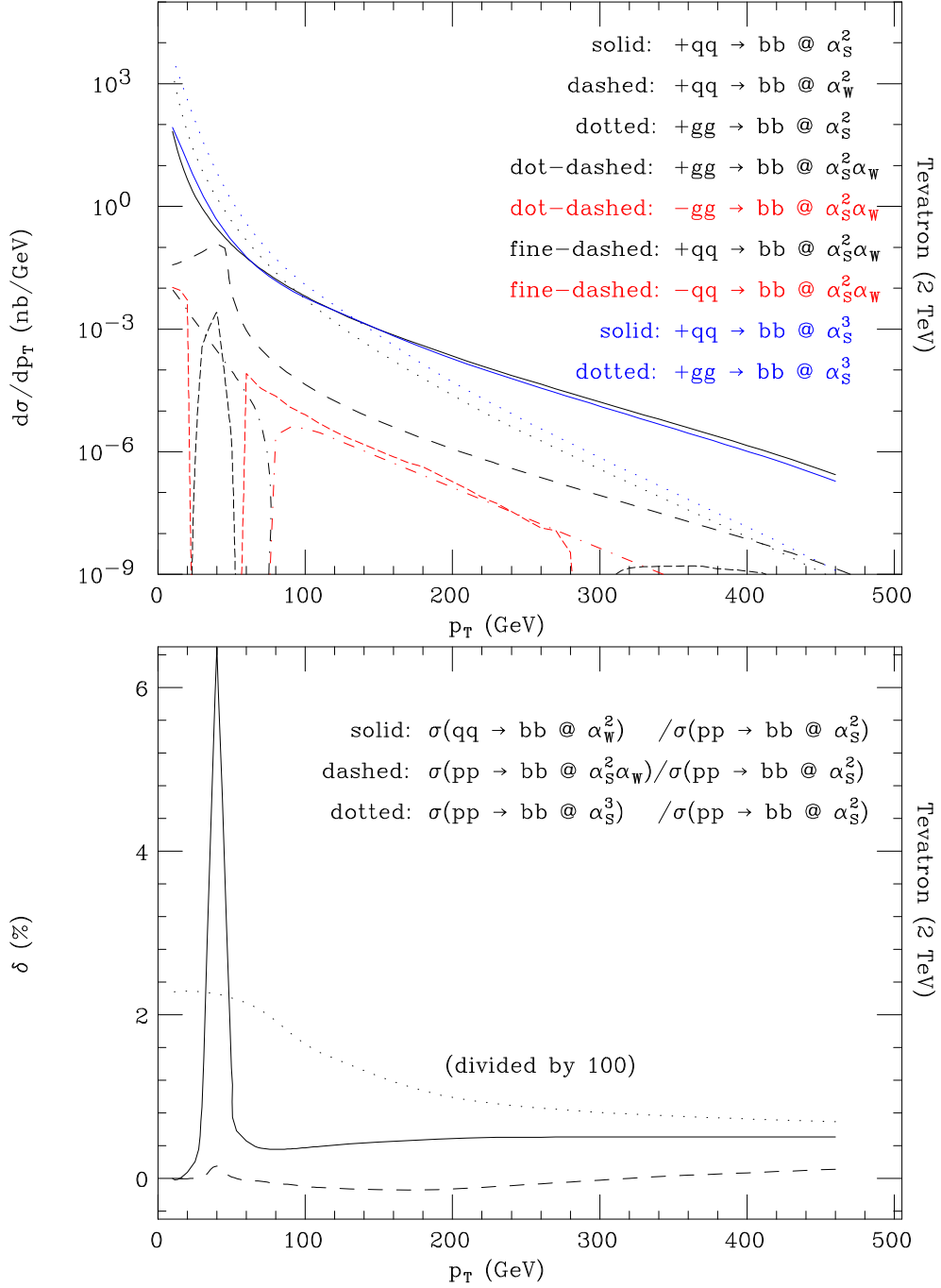


Figure 1: The total cross section contributions vs. the transverse momentum of the  $b$ -jet for  $p\bar{p} \rightarrow b\bar{b}$  production at Tevatron (2 TeV) as obtained via the various subprocesses discussed in the text (top) and the corrections due to the  $\alpha_{EW}^2$ ,  $\alpha_S^2 \alpha_{EW}^2$  and  $\alpha_S^3$  terms relative to the  $\alpha_S^2$  ones (bottom).

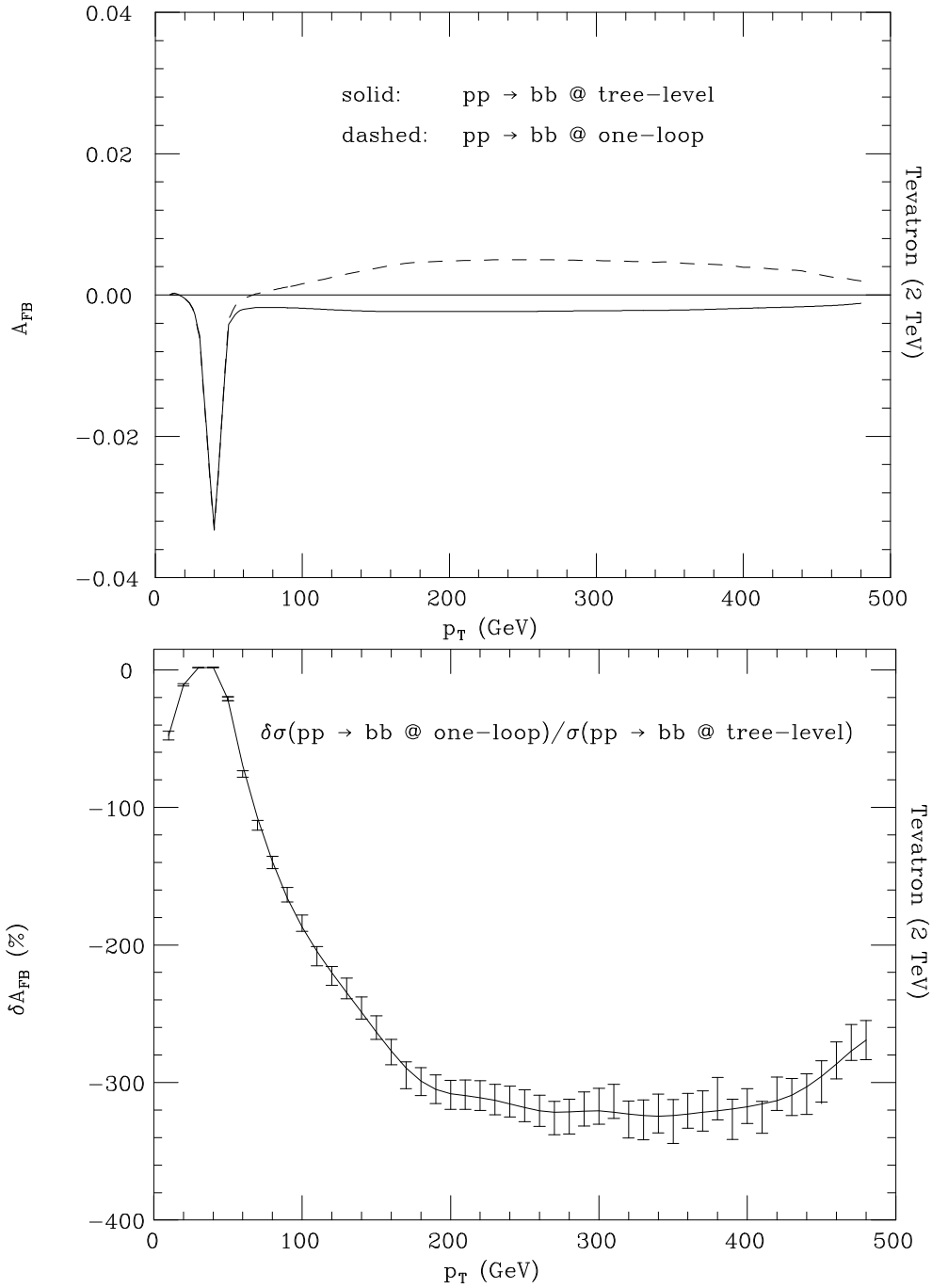


Figure 2: The forward-backward asymmetry vs. the transverse momentum of the  $b$ -jet for  $p\bar{p} \rightarrow b\bar{b}$  events at Tevatron (2 TeV), as obtained at tree-level and one-loop order (top) and the relative correction of the latter to the former (bottom). (Errors in the ratio are statistical.)

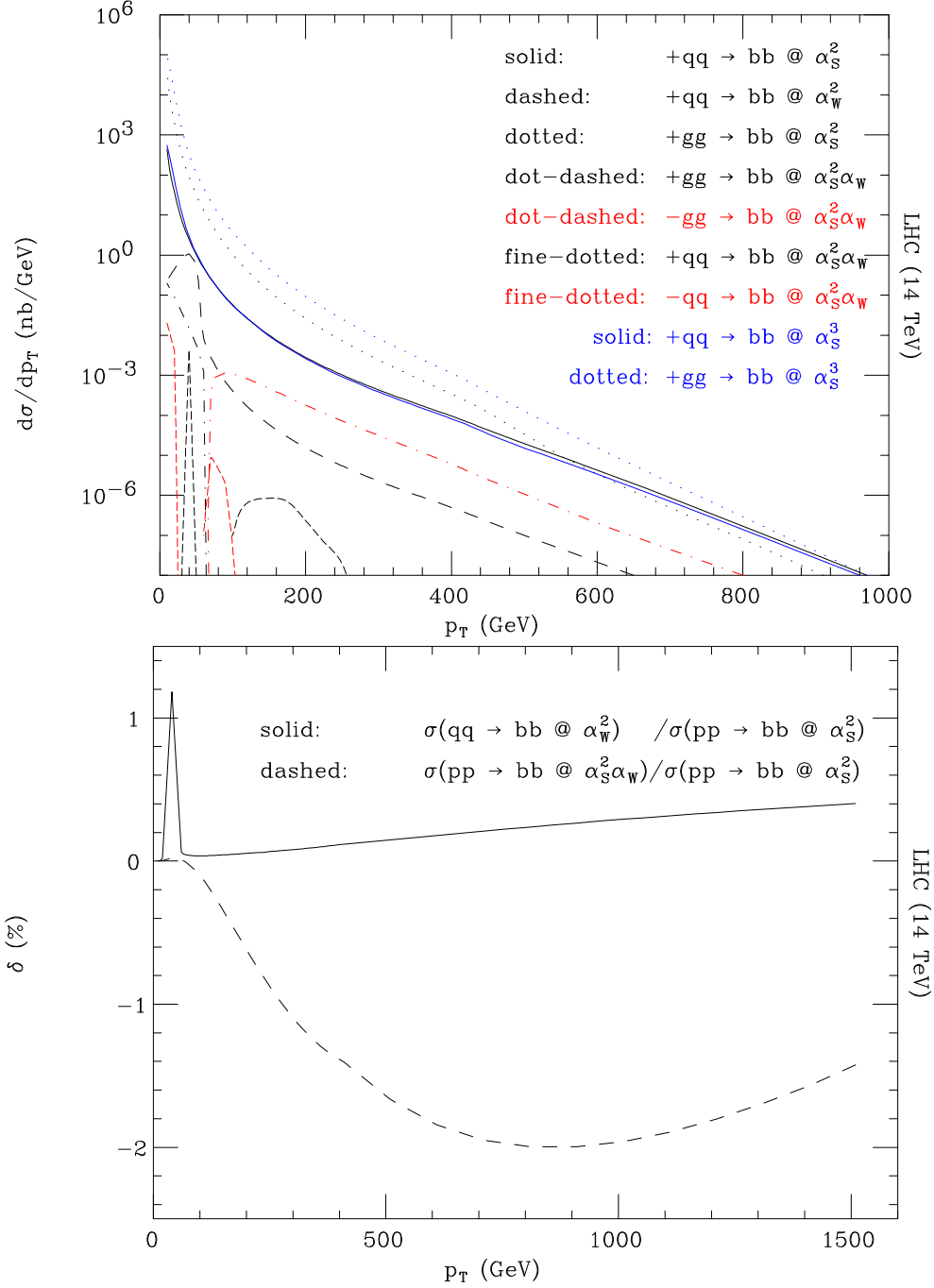


Figure 3: The total cross section contributions vs. the transverse momentum of the  $b$ -jet for  $pp \rightarrow b\bar{b}$  production at LHC (14 TeV) as obtained via the various subprocesses discussed in the text (top) and the corrections due to the  $\alpha_{EW}^2$  and  $\alpha_S^2 \alpha_{EW}^2$  terms relative to the  $\alpha_S^2$  ones (bottom). (Here, we do not show the corrections due to  $\alpha_S^3$  terms as results are perturbatively unreliable, given that  $K$ -factors as large as 3–4 can appear.)